Uniaxial-stress effect of the EPR spectra of magnetic impurities in $SrCl_2$

J. Groen, G. van Opbroek, K. Post, and H. W. den Hartog
Solid State Physics Laboratory, University of Groningen, 1 Melkweg, 9718-EP Groningen, The Netherlands
(Received 23 April 1984)

In this paper we present the results of uniaxial-stress-effect experiments in EPR on $SrCl_2$ crystals doped with different kinds of magnetic impurities: Mn^{2+}, Co^{2+}, and Eu^{2+}. The impurities Mn^{2+} and Co^{2+} are appreciably smaller than the cation (Sr^{2+}) of the host crystal, whereas Sr^{2+} and Eu^{2+} have about the same size. It appears that the uniaxial-stress effect of the smaller-sized impurities is much larger than expected on the basis of the elastic properties of the $SrCl_2$ single crystal. Local deformations in the neighborhood of these impurities play a decisive role. Earlier electric-field-effect experiments carried out in our laboratory have shown that substitutional Mn^{2+} impurities in $SrCl_2$ are located in a rather shallow potential well, which can be modified significantly by means of an external electric field. This observation is supported by the behavior of the crystal-field splitting and the uniaxial-stress effect as a function of the temperature observed in the present investigation.

I. INTRODUCTION

We have demonstrated in earlier papers that small-sized magnetic impurities such as Mn^{2+} and Co^{2+} in $SrCl_2$ behave in a rather unusual way if an external electric field is applied to the single crystal.[1,2] In EPR we have observed that as a result of the electric field the symmetry of the site associated with the magnetic impurity is lowered from cubic (O_h) to axial or even orthorhombic (for Co^{2+}). In order to understand the observations we have to assume that the impurities move away from the substitutional position under the influence of the external electric field. The observations for Co^{2+} are even more complicated; here in some cases there is an additional lowering of the symmetry which may be due to a more complicated relaxation of the nonspherical ion in the host crystal.[2] It has been shown that the displacements induced by the external electric field are orders of magnitude larger than those estimated from the ionic polarization properties of normal ionic materials.

We have proposed that the remarkable results should be explained by assuming that the potential well seen by the above-mentioned impurity is very flat; this implies that we are dealing with loosely bound impurities. In order to check the experimental results we have carried out theoretical cations of the system $SrCl_2$:Mn^{2+} which have indeed shown that the potential well of Mn^{2+} in $SrCl_2$ is very flat, and, in addition, that it has significant contributions from anharmonic terms.[3] More recent calculations carried out in this laboratory by Hess and den Hartog[4] support the model outlined above. From these calculations we have found that the relaxations of the ions neighboring the central Mn^{2+} impurity are appreciable and should not be ignored.

A method to study the behavior of these ions and the remaining crystal is the uniaxial-stress experiment in EPR. We have applied uniaxial stress along the principal crystallographic directions in order to obtain additional information about the Mn^{2+} center in $SrCl_2$. Because interesting variations have been observed in electric-field-effect (EFE) experiments in the temperature range 4—300 K, we have carried out uniaxial-stress experiments in the same temperature region. From the results obtained from these experiments we conclude that the potential well of Mn^{2+} in $SrCl_2$ is indeed very flat. We can also deduce from the stress results that there is an appreciable anharmonic contribution which causes the potential well to have an approximate shape, as shown in Fig. 1.

The stress results cannot be explained on the basis of the bulk properties of the $SrCl_2$ crystal. If we employ the elastic properties of $SrCl_2$ [which have been determined in the temperature range 4—300 K (Ref. 5) to calculate the observed uniaxial-stress effect, we find uniaxial-stress effects which are much smaller than those observed experimentally. The predicted uniaxial-stress effects along $\langle 111 \rangle$ and $\langle 110 \rangle$, in particular, vary by more than an order of magnitude. From theoretical calculations carried out by Hess and den Hartog,[4] we know that the potential wells associated with the eight Cl^- ions neighboring the Mn^{2+} impurity are shallower than those for the unperturbed Cl^- ions, indicating that the local elastic constants

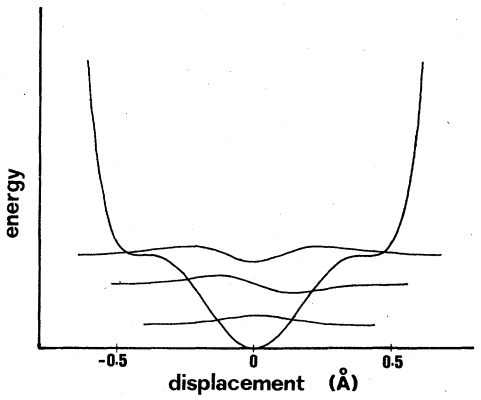

FIG. 1. Shape of the potential well of a manganese impurity in $SrCl_2$ as taken from the electric-field-effect experiments carried out by Roelfsema and den Hartog (Refs. 1 and 2).

are smaller than the bulk values.

In order to explain the observations made for $SrCl_2:Mn^{2+}$ we have to assume that the local elastic constant c_{44} associated with the above-mentioned eight Cl^- ions is smaller than the bulk value by a factor of about $\frac{1}{5}$. For the remaining ions in the crystal we take the normal parameter c_{44}. The local elastic constants c_{11} and c_{12} are assumed to be approximately equal to the bulk values. It should be emphasized here that the model used for the description of the uniaxial-stress results is a very crude one because we did not take into account the effect of the large displacements of the first coordination shell on the displacements of ions in further shells.

A situation similar to that of $SrCl_2:Mn^{2+}$ has been observed for the system $SrCl_2:Co^{2+}$. There is, however, one major difference between these two impurity systems. The uniaxial-stress effect observed for $SrCl_2:Co^{2+}$ is much larger than in $SrCl_2:Mn^{2+}$. Whereas maximum splittings for $SrCl_2:Mn^{2+}$ observed in our experiments are approximately 100 G, the corresponding splitting for $SrCl_2:Co^{2+}$ is a *few thousand* G. These very large splittings can be explained by using the energy-level scheme of divalent cobalt with tetrahedral symmetry. In addition, we note that the anharmonic contributions to the potential well of the Co^{2+} ion are probably larger than for $SrCl_2:Mn^{2+}$ because the difference between the ionic radii of Sr^{2+} and Co^{2+} is larger than that for Sr^{2+} and Mn^{2+}.

The results obtained for $SrCl_2:Mn^{2+}$ and $SrCl_2:Co^{2+}$ are compared with those for $SrCl_2:Eu^{2+}$. The ionic radius of Eu^{2+} is approximately equal to that of Sr^{2+}. Both the magnitude of the stress-induced crystal-field parameters and the temperature dependence of these parameters can be understood in terms of the elastic properties of the bulk $SrCl_2$ crystal. This indicates that the deviations observed for $SrCl_2:Mn^{2+}$ and $SrCl_2:Co^{2+}$ are related to the deviations between the ion sizes of the impurity and the host-lattice ions.

II. EXPERIMENTAL PROCEDURES

The crystals employed in this investigation were grown by means of a modified Bridgman method. The samples were grown using $SrCl_2 \cdot 6H_2O$ (British Drug House, for atomic absorption spectroscopy). Before crystal growth the raw materials were dehydrated in a quartz tube by heating the powder very carefully under vacuum at increasing temperatures up to about 150 °C. This treatment usually takes 24—48 h. After finishing the dehydration the powder was heated to temperatures well above the melting point and flushed with a mixture of pure and water-free argon gas and CCl_4 vapor. This mixture drastically reduces the OH^-- and O^{2-}-impurity contents in the melt. Usually, this type of treatment takes a few hours. After finishing this purification procedure the temperature was allowed to decrease to approximately room temperature, the system was evacuated again, and the quartz tube was sealed.

Two or three sealed quartz tubes were introduced simultaneously in a Bridgman-type furnace with a steep temperature gradient at approximately the melting point of $SrCl_2$. The quartz tubes were lowered in the region of the temperature gradient at a rate of 2—4 mm/h in order to obtain high-quality single-crystalline materials. After this, the samples were cooled down very slowly to room temperature over a period of 24—48 h.

The impurities were added to the $SrCl_2 \cdot 6H_2O$ in concentrations of $(1-4)\times 10^{-2}$ mol %. These concentrations are sufficient to ensure reasonable signal intensities. Higher concentrations led to broadening of the EPR lines, leading in turn to a reduced accuracy of the stress-induced crystal-field parameters.

The EPR experiments were carried out with an *X*-band Varian Associates spectrometer *E*-line Century Series which was extended with a data-acquisition system. The results were analyzed with a Hewlett Packard HP 9835 computer.

Uniaxial stress was applied to the crystal by means of a setup similar to the one described by Szumowski and Falkowski.[6] Pressures up to 10 kg/cm^2 were applied to a quartz anvil with a diameter of 30 mm. As the surface area of the crystal is less than 2 mm^2, with this setup we were able to reach uniaxial-stress intensities up to 1000 bars.

The experiments were carried out between 4 K and room temperature employing a liquid-He-flow cryostat which was inserted into the microwave cavity.

The sample temperature was measured with a calibrated thermocouple which was introduced into the cavity together with the uniaxial-stress equipment. The stress setup was able to be mounted easily, so that the sample and the thermocouple were approximately at the center of the microwave cavity.

III. EXPERIMENTAL RESULTS

A. $SrCl_2:Mn^{2+}$

The *X*-band EPR spectra for $SrCl_2:Mn^{2+}$ samples were recorded in the temperature range 20—200 K. In Fig. 2 we present a spectrum measured at 77 K, with $\vec{H}_0$ lying in the (111) plane. In this case we have not applied any uniaxial stress to the crystal. We observe six groups of lines, with different shapes. Some of the groups show strongly overlapping lines, other are relatively well resolved. The main splitting of the spectrum is associated with hyper-

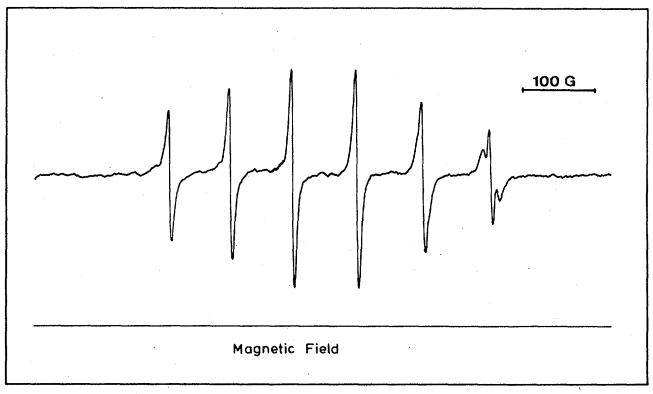

FIG. 2. EPR spectrum of a single crystal of the type of $SrCl_2:Mn^{2+}$ at 77 K; $\vec{H}_0$ is lying in a (111) plane, and the uniaxial stress is 0.

fine interaction between the $3d^5$-electron system and the nuclear spin of the manganese ion. The splitting is isotropic and has a value of 88 G. Each of the individual groups consists of five lines; the splitting is caused by (i) second-order hyperfine splitting, and (ii) the cubic crystal-field potential. Because, in general, the second-order hyperfine-interaction splitting is not the same for each of the M_I groups (M_I is the quantum number associated with the nuclear spin $\vec{I}$) and the crystal-field interaction is rather weak, the shapes of the groups of five lines are different from one another.

The application of uniaxial stress leads to a stronger splitting of the individual groups of lines. In the extreme case all the groups are well resolved and in some cases the lines of neighboring groups partly overlap. In Fig. 3 we show the EPR spectrum of a sample with a uniaxial stress of 500 bars along the [111] direction; the magnetic field direction is in the (111) plane.

In order to study the temperature dependence of the uniaxial-stress effect we also need information about the temperature dependence of the EPR transitions as a function of the temperature. From the results presented in Fig. 4 we see that the width of the EPR lines decreases with decreasing temperature; in addition, we see that the splitting of the lines increases with decreasing temperature. A complete survey of the behavior of the splitting as a function of temperature has been given in Fig. 5. The figure shows a strong increase for the splitting between 30 and 60 K. The origin of this variation is probably the variation of the crystal-field—interaction parameter, which has significant thermal contributions. These contributions have for Mn^{2+}, been discussed by Pfister, Dreybrodt, and Assmus.[7] These authors found small thermal contributions for the charge-compensation complex consisting of a divalent Mn^{2+} ion and a cation vacancy in NaCl and LiCl. The present experimental results show that the variations of the line positions for $SrCl_2$:Mn^{2+} are much larger than those found by Pfister *et al.*[7] In addition, we find that at high temperatures the shift with varying temperatures is much smaller than in the temperature range 30—70 K.

If one applies uniaxial stress the behavior of the splitting between the $S_z=-\frac{3}{2}\rightarrow-\frac{1}{2}$ and the $S_z=\frac{1}{2}\rightarrow\frac{3}{2}$ transitions behaves quite differently as a function of the temperature. In Fig. 6 we show the behavior of the above-mentioned splitting as a function of T for a few different values of the uniaxial stress. We observe that the splitting increases with increasing applied stress; from

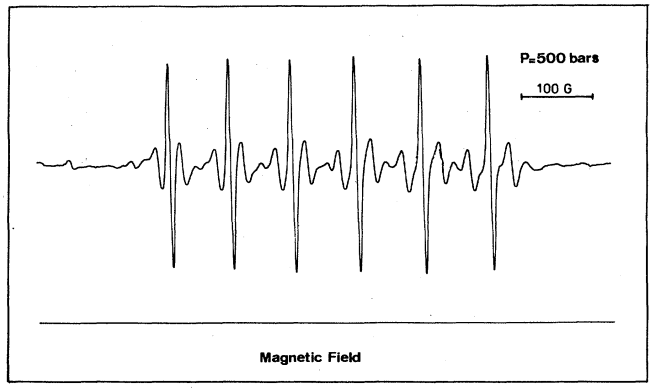

FIG. 3. EPR spectrum of a $SrCl_2$:Mn^{2+} crystal measured at 77 K with $\vec{H}_0$ lying in a (111) plane, and the uniaxial stress is 500 bars.

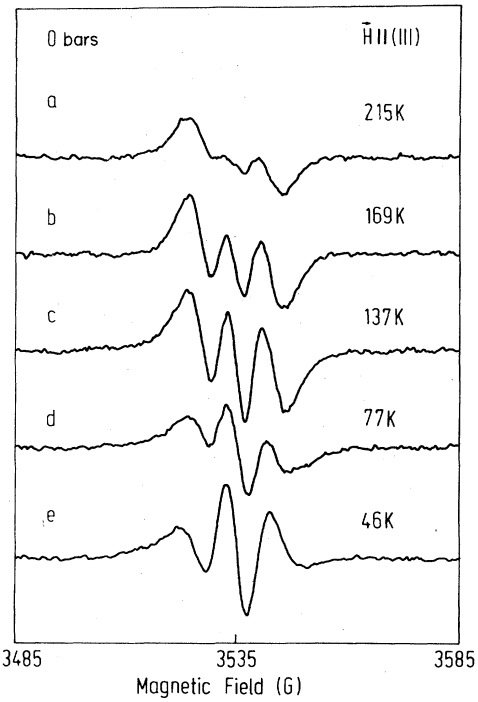

FIG. 4. Behavior of the high-field quintet ($M_I=\frac{5}{2}$) as a function of the temperature. The magnetic field direction $\vec{H}_0$ is parallel to the (111) plane, and the applied stress is 0.

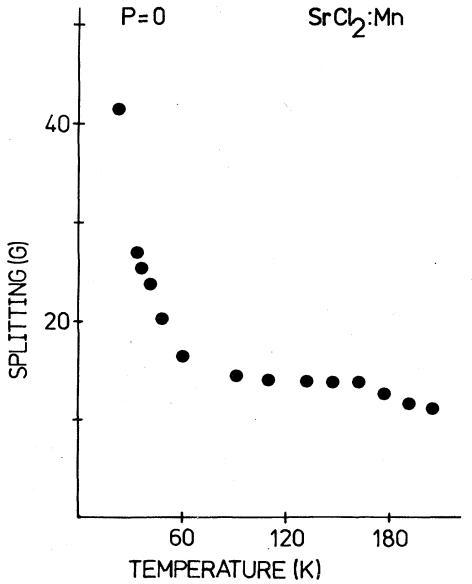

FIG. 5. Behavior of the splitting between the $S_z=\frac{3}{2}\leftrightarrow\frac{1}{2}$ and the $S_z=-\frac{1}{2}\leftrightarrow-\frac{3}{2}$ transitions of the $M_I=\frac{5}{2}$ quintet as a function of the temperature; the applied stress is 0.

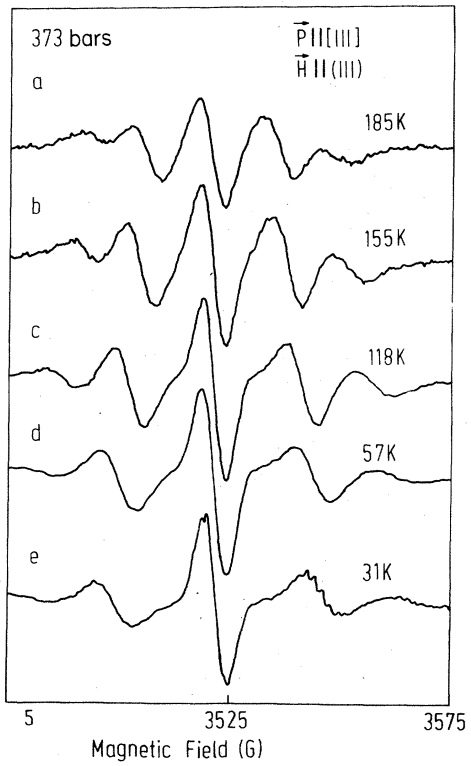

FIG. 6. Behavior of the splitting between the $S_z=\frac{3}{2}\leftrightarrow\frac{1}{2}$ and the $S_z=-\frac{1}{2}\leftrightarrow-\frac{3}{2}$ transition as a function of the temperature. The magnetic field direction $\vec{H}_0$ is parallel to the (111) plane, and the uniaxial stress (373 bars) has been applied along the [111] direction.

a comparison of the results presented in Fig. 5 and those in Fig. 6, we find that the uniaxial-stress effect depends upon the temperature. The net stress effect as a function of T has been given in Fig. 7.

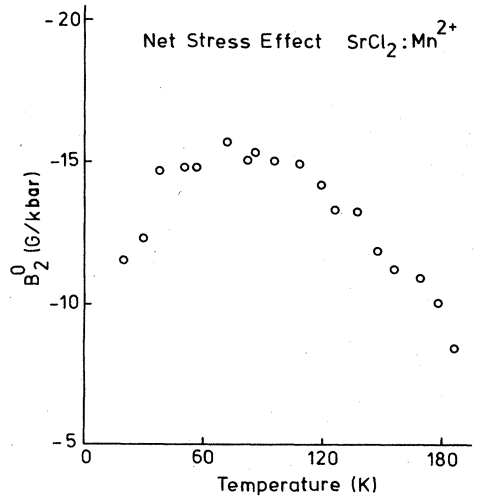

FIG. 7. Behavior of the net uniaxial-stress effect as a function of the temperature.

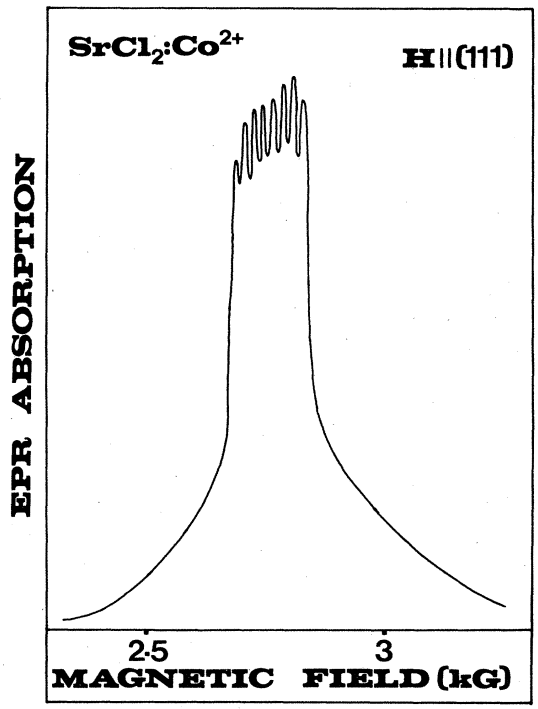

FIG. 8. EPR signal of a $SrCl_2:Co^{2+}$ crystal.

B. $SrCl_2:Co^{2+}$

The EPR spectrum of Co^{2+} in $SrCl_2$ can be observed only for temperatures below about 10 K. This is due to the fact that the relaxation time decreases very rapidly with increasing temperature. The spectra of $SrCl_2:Co^{2+}$ samples can be conveniently recorded at 4.2 K. An example has been shown in Fig. 8; the spectrum consists of eight lines which are approximately equidistant. This splitting is associated with the interaction between the paramagnetic electron system and the nuclear spin of the cobalt ion, which has a value of $S=\frac{7}{2}$. A more complete description of the spectrum of unperturbed Co^{2+} in $SrCl_2$ has been given by Roelfsema and den Hartog.[2] The parameters occurring in the spin Hamiltonian as derived from the experimental results of the present study agree well with those given by Roelfsema and den Hartog.[2]

The spectrum given in Fig. 8 only shows the $S_z=-\frac{1}{2}\rightarrow\frac{1}{2}$ transition; the $\pm\frac{3}{2}\rightarrow\pm\frac{1}{2}$ transitions cannot be observed because they are hidden underneath the $S_z=-\frac{1}{2}\rightarrow\frac{1}{2}$ transition. The crystal field associated with the cubic surroundings does not influence the positions of the $S_z=\pm\frac{3}{2}\rightarrow\pm\frac{1}{2}$ transitions because the ground state of the Co^{2+} $3d$-electron system can be described by an effective $S=\frac{3}{2}$ state, and, consequently, the terms $B_4^mO_4^m$ and $B_6^mO_6^m$ in the spin Hamiltonian do not contribute to the splitting of the ground-state quartet. On the other hand, the terms $B_2^mO_2^m$ do not appear in a spin Hamiltonian with cubic symmetry. These contributions only appear for symmetries lower than cubic.

If we apply uniaxial stress the spectrum shows an additional splitting; the individual hyperfine lines are

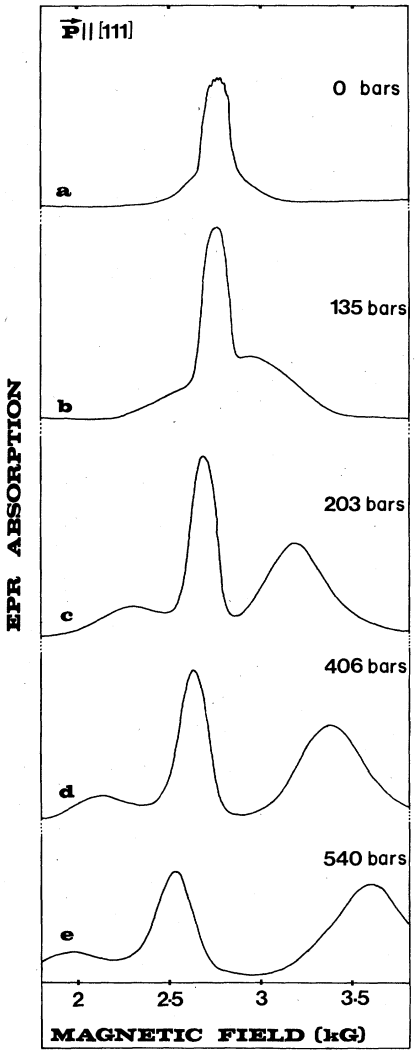

FIG. 9. EPR signals of a $SrCl_2$:Co^{2+} crystal, observed if uniaxial stress is applied along the [111] direction. With increasing uniaxial stress the splitting increases drastically.

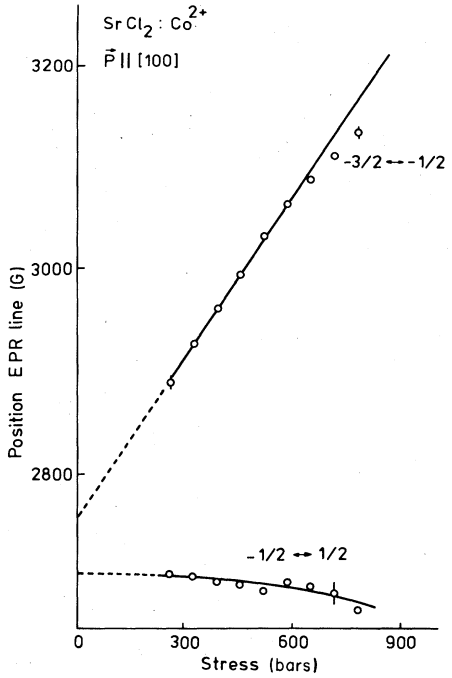

FIG. 10. Behavior of the $S_z=-\frac{3}{2}\leftrightarrow-\frac{1}{2}$ and the $S_z=-\frac{1}{2}\leftrightarrow\frac{1}{2}$ transitions of $SrCl_2$:Co^{2+} as a function of the uniaxial stress. The $S_z=\frac{1}{2}\leftrightarrow\frac{3}{2}$ transition could not be located with sufficient accuracy because it was hidden underneath the $S_z=-\frac{1}{2}\leftrightarrow\frac{1}{2}$ transition.

broadened to such an extent that only the three fine transitions, $S_z=-\frac{3}{2}\rightarrow-\frac{1}{2}$, $-\frac{1}{2}\rightarrow\frac{1}{2}$, and $\frac{1}{2}\rightarrow\frac{3}{2}$, are resolved. An example of the spectra obtained during the application of uniaxial stress is given in Fig. 9. The stress has been applied along the crystallographic [111] direction and the magnetic field direction is in the (111) plane. The stress-induced crystal-field splitting is much larger for $SrCl_2$:Co^{2+} than for $SrCl_2$:Mn^{2+} (see also Fig. 3). Another feature of the results is that the intensity ratio of the fine transition deviates considerably from that expected, 3:4:3. Part of the deviation is due to the population differences related to the Boltzmann distribution. Another part is ascribed to second-order effects of the transition probabilities. These have been calculated recently by Harris and Tucker.[8] The two mechanisms are, however, *insufficient* to describe the observed variations of the intensity ratio. It appears that a detailed investigation of the development of the intensity ratios as a function of the strength of the uniaxial stress is necessary.

The variations of the uniaxial-stress effect of $SrCl_2$:Co^{2+} as a function of the orientation has been investigated for $\vec{P}//[111]$ and $\vec{H}_0$ lying in the (111) plane, and it turns out that the stress effect is axially symmetric for rotations about the [111] crystal axis. This result is in agreement with what is expected on the basis of the deformation properties of the $SrCl_2$ crystal.

In Fig. 10 we present the uniaxial-stress results for experiments with $\vec{P}//[100]$ and $\vec{H}_0$ lying in the (100) plane. The splitting does not increase as drastically with the magnitude of $\vec{P}$ as in the [111] experiment. The variations of the $S_z=\frac{1}{2}\rightarrow\frac{3}{2}$ and $-\frac{3}{2}\rightarrow-\frac{1}{2}$ transitions are approximately linear with P; in the high-stress range, however, we observed in all our experiments (for $\vec{P}//[100]$) significant deviations from this linear relationship. Here too the splitting appears to be axially symmetric, now for rotation of the sample about the stress direction ([100]) as well. If uniaxial stress is applied along the [110] direction and the magnetic field direction is chosen in the (110) plane, we observe strong deviations from axial symmetry. This agrees with our expectations on the basis of the knowledge of the elastic properties of $SrCl_2$. The result of uniaxial-stress experiments with $P=610$ bars along [110] and with $\vec{H}_0$ lying in the (110) plane has been given in Fig. 11. The rotational diagram, obtained during rotation about the stress axis ([110]), is presented in Fig. 12. This rotational diagram shows that

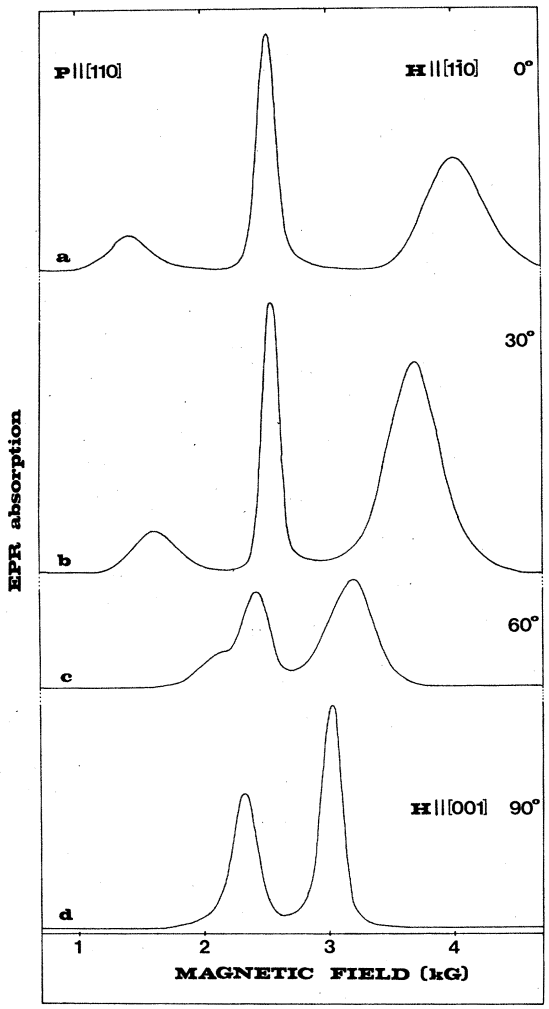

FIG. 11. EPR signals observed for $SrCl_2:Co^{2+}$ if a uniaxial stress of 610 bars is applied along the [110] direction. The different signals are obtained after rotations of the crystal about the [110] axis.

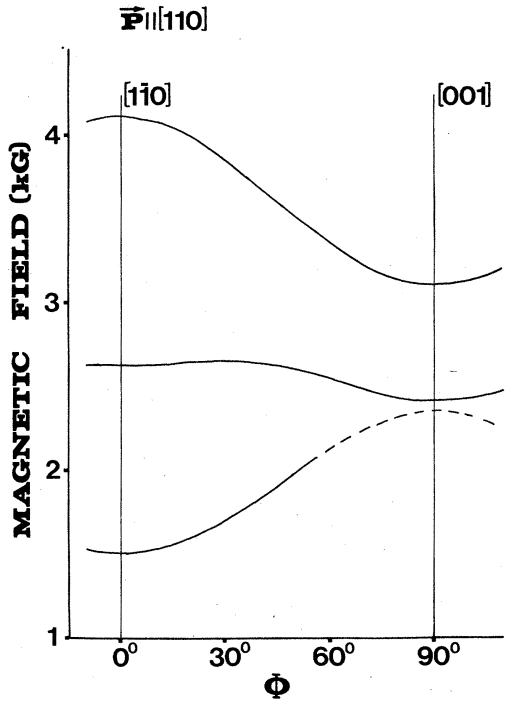

FIG. 12. Rotational diagram of the EPR signal of $SrCl_2:Co^{2+}$ (with a stress of 610 bars along the [110] direction), obtained for a rotation about the [110] axis.

the splitting for $\vec{P}$//[110] has a maximum value for $\vec{H}_0$//[1$\bar{1}$0] and a minimum for $\vec{H}_0$//[001]. From this diagram we can derive the important stress-induced crystal-field parameters.

From the above-described experiments we were able to calculate, for all different types of experiments, the stress-induced crystal-field parameters. These parameters have been compiled in Table I. We note that only the results obtained with $\vec{P}$//[111] and $\vec{P}$//[100] yield independent parameters. The parameters found from the experiment with $\vec{P}$//[110] can be predicted using the values obtained from the [111] and [100] experiments. The latter results have been included in Table I in order to make a comparison possible.

C. $SrCl_2:Eu^{2+}$

Eu^{2+} has a $4f^7$ ground state, which is usually referred to as the $^8S_{7/2}$ state. The EPR signal of this impurity shows a crystal-field splitting into seven fine lines. In addition, there is a hyperfine splitting due to the interaction between the electron system and the nuclear spin of the Eu^{2+} ion. Natural Eu has two magnetic isotopes, ^{153}Eu and ^{155}Eu, both with $I=\frac{5}{2}$. In order to simplify the interpretation we have prepared samples of $SrCl_2$ doped with only one isotope (^{153}Eu). For these samples the signal generally consists of seven groups of six equidistant lines; the splitting within the groups is due to contact interaction between the ground-state electrons with the magnetic ^{153}Eu nucleus.

In Fig. 13 we show the EPR signals of $SrCl_2:^{153}Eu^{2+}$ with and without uniaxial stress. The stress direction is [1$\bar{1}$0] and the magnetic field is along [111]; the upper trace was recorded with $P=0$ bars and the lower signal was taken with $P=300$ bars. Both experiments have been carried out at 50 K. From Fig. 13 we see that the stress-induced shifts are comparable to those observed for $SrCl_2:Mn^{2+}$. In addition, we find that the lines of the

TABLE I. Experimental stress-induced crystal-field parameters ($SrCl_2:Co^{2+}$).

Stress axis	B_2^0 (G/kbar)	B_2^2 (G/kbar)
[100]	−286	0
[110]	−437	252
[111]	−507	0

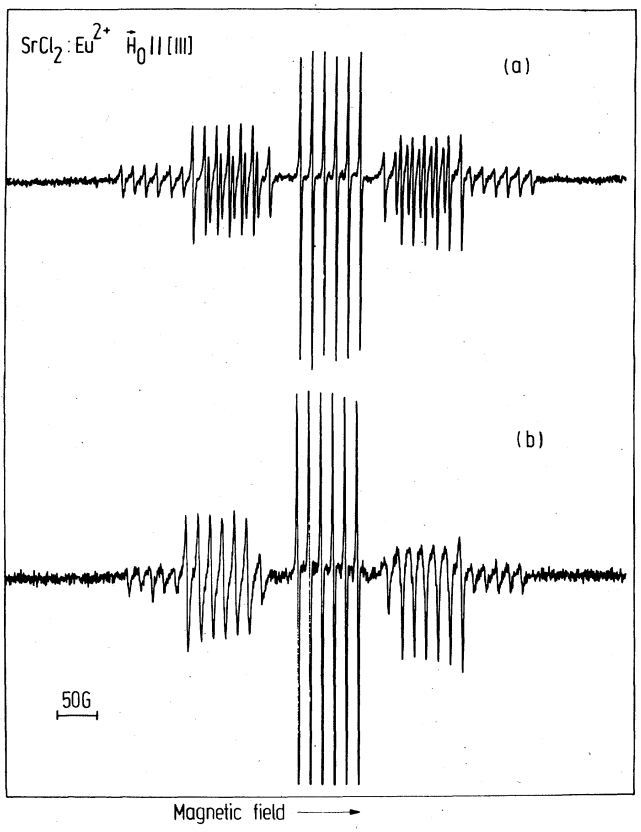

FIG. 13. EPR signal of $SrCl_2$:$^{153}Eu^{2+}$ single crystal. The magnetic field is along the [111] direction. The upper signal [part (a)] has been obtained with zero stress; the lower trace [part (b)] has been recorded with a stress of 300 bars along [1$\bar{1}$0] direction.

lower spectrum are broadened, just as in the case of $SrCl_2$:Mn^{2+}. It should be noted, however, that, in principle, divalent Eu is much more sensitive to electrostatic effects than Mn^{2+}, as will be discussed later in this paper.

We have also studied the temperature dependence of the uniaxial-stress effect of $SrCl_2$:Eu^{2+}. This can be done rather easily because, just as in the case of Mn^{2+}, we are dealing with an S-state ion. From these experiments we found that the uniaxial-stress effect is approximately constant in the temperature range between 20 and 150 K. At 77 K we find for the uniaxial-stress effect of $SrCl_2$:Eu^{2+} the following results: $C_{11}=\pm(1\pm1)$ G/kbar and $C_{44}=\mp(9\pm3)$ G/kbar.

IV. DISCUSSION

A. $SrCl_2$:Mn^{2+}

In both $SrCl_2$:Mn^{2+} and $SrCl_2$:Co^{2+} we have observed anomalously large uniaxial-stress effects in EPR which cannot be explained on the basis of the bulk elastic properties of the pure $SrCl_2$ crystal. These anomalous uniaxial-stress effects are in line with the results of electric-field-effect measurements carried out earlier in this laboratory.[1,2] We have observed very large electric field effects which could not be explained by assuming the normal shifts of the ions in the crystal as a result of the external electric field. For $SrCl_2$:Mn the estimated shift of the central Mn^{2+} impurity for an electric field strength of about 20 kV/mm is 0.1—0.2 Å.

From the electric-field-effect experiments we have concluded that the Mn^{2+} impurity in $SrCl_2$ "feels" a slowly varying potential from the rest of the surrounding crystal. In addition, the results obtained for the temperature dependence of the electric field effect support this interpretation (see Ref. 1). In this paper we present new results for the behavior of the fine splitting as a function of the temperature. We have seen that this splitting increases drastically with decreasing temperature below approximately 70 K. The observed temperature dependence is anomalous from two points of view. First, the magnitude of the effect below 70 K is much larger than what is observed normally.[7] Second, the variations of the splitting as a function of the temperature are relatively small for temperatures >70 K. This is in contrast with the expected behavior of vibrational contributions to the crystal-field splitting, which can be written as (see Ref. 7)

$$D(T)=D_0+D\coth(\hbar\omega/2k_BT)\ . \tag{1}$$

This means that the observed behavior of the crystal-field splitting should be explained in an alternative way. The most obvious explanation is again in line with the anharmonic potential well proposed by us in an earlier paper[2] (see Fig. 1). At relatively low temperatures an appreciable part of the Mn^{2+} ions is in the vibrational states situated in the deepest part of the potential well. If the temperature is increased, however, higher vibrational levels are occupied. As a result of the anharmonic shape of the potential well, the wave function of the Mn^{2+} ion is displaced considerably from the equilibrium position. As a result the vibrational contribution to the crystal-field-splitting parameter increases rapidly with T. If the temperature is increased further the influence of the anharmonic part of the potential well is reduced, and at sufficiently high temperatures the normal behavior of the vibrational contributions is obtained. This is indeed what has been observed experimentally. For $T>70$ K the variation of the crystal-field splitting as a function of T is much smaller than in the temperature region $T<60$ K.

The uniaxial-stress results show that there is a broad maximum for temperatures of about 70 K. The position of this maximum is approximately the same as for the electric-field-effect experiments observed by Roelfsema and den Hartog.[1] This behavior can be explained easily by considering the small-sized impurity ion in the $SrCl_2$ lattice. At low temperatures the Mn^{2+} ion is localized at the center of the substitutional site. The repulsive forces between this ion and the surrounding Cl^- ions are weak; therefore the uniaxial-stress effect, which is determined for a significant part by the motion of the nearest neighbors, is relatively large. At high temperatures on the other hand, the amplitude of the vibrations of the Mn^{2+} ion is large, leading to a reduction of the distortions of the first coordination shell with Cl^- ions.

There are several possible ways to describe the uniaxial-stress results. Until now we have been looking at

shifts of the EPR lines as a function of the magnitude and direction of the uniaxial stress. We can describe each of the experiments with two stress-induced crystal-field parameters, B_2^0 and B_2^2. A difficulty with this method is, however, that the values of B_2^0 and B_2^2 depend upon the stress direction. For the description of all stress-effect experiments there are only two independent parameters from which we can derive the second-degree crystal-field parameters for all stress directions. In the literature these parameters are referred to as C_{11} and C_{44}, analogous to the elastic constants c_{11} and c_{44}.

Schulman *et al.*[9] have shown that the behavior of the zero-field splitting induced by uniaxial stress can be written in a form similar to the generalized Hooke's law for the elastic properties of cubic crystals. Rosenvasser Feher[10] has pointed out that in magnetic resonance C_{12} is not an independent parameter because $C_{12}=-\frac{1}{2}C_{11}$. In general, we can write the stress-induced crystal-field Hamiltonian as

$$\mathcal{H}_{\text{stress}}=\sum_{i,j=1}^{3} S_i D_{ij} S_j \ , \tag{2}$$

where S_i and S_j are the spin operators S_x, S_y, and S_z; D_{ij} are the various zero-field-splitting parameters. As mentioned above, for a cubic crystal we can derive the following relation between the stress-induced zero-field-splitting parameters D_{ij} and stresses X_{ij}:

$$\begin{bmatrix} D_{11} \\ D_{22} \\ D_{33} \\ D_{12} \\ D_{23} \\ D_{31} \end{bmatrix} = \begin{bmatrix} C_{11} & -\frac{1}{2}C_{11} & -\frac{1}{2}C_{11} & 0 & 0 & 0 \\ -\frac{1}{2}C_{11} & C_{11} & -\frac{1}{2}C_{11} & 0 & 0 & 0 \\ -\frac{1}{2}C_{11} & -\frac{1}{2}C_{11} & C_{11} & 0 & 0 & 0 \\ 0 & 0 & 0 & C_{44} & 0 & 0 \\ 0 & 0 & 0 & 0 & C_{44} & 0 \\ 0 & 0 & 0 & 0 & 0 & C_{44} \end{bmatrix} \begin{bmatrix} X_{11} \\ X_{22} \\ X_{33} \\ X_{12} \\ X_{23} \\ X_{31} \end{bmatrix} . \tag{3}$$

Using (3) we can rewrite (2) in the following form:

$$\begin{aligned}\mathcal{H}_{\text{stress}}=&\, C_{11}\{[X_{11}-\tfrac{1}{2}(X_{22}+X_{33})]S_x^2+[X_{22}-\tfrac{1}{2}(X_{33}+X_{11})]S_y^2+[X_{33}-\tfrac{1}{2}(X_{22}+X_{11})]S_z^2\} \\ &+C_{44}[X_{12}(S_xS_y+S_yS_x)+X_{13}(S_xS_z+S_zS_x)+X_{23}(S_yS_z+S_zS_y)] \ .\end{aligned} \tag{4}$$

We can now derive the relations for the stress-induced spin Hamiltonian for the most important directions, ⟨100⟩, ⟨110⟩, and ⟨111⟩,

$$\begin{aligned}\langle 100\rangle \cdots \mathcal{H}_{\text{stress}}^{\langle 100\rangle}&=\tfrac{1}{2}PC_{11}[3S_z^2-S(S+1)] \ , \\ \langle 110\rangle \cdots \mathcal{H}_{\text{stress}}^{\langle 110\rangle}&=-\tfrac{1}{4}PC_{11}[3S_z^2-S(S+1)] \\ &\quad +\tfrac{1}{2}PC_{44}[\tfrac{1}{2}(S_+^2-S_-^2)] \ , \\ \langle 111\rangle \cdots \mathcal{H}_{\text{stress}}^{\langle 111\rangle}&=\tfrac{1}{3}PC_{44}(S_xS_y+S_yS_x+S_xS_z \\ &\quad +S_zS_x+S_yS_z+S_zS_y) \ .\end{aligned} \tag{5}$$

In Eq. (5) the principal axes $\vec{x}$, $\vec{y}$, and $\vec{z}$ are along the crystallographic [100], [010], and [001] directions, respectively. The results of the experiments with the stress along [110] and [111] should be written in terms of a rotated frame of axes $\vec{x}'$, $\vec{y}'$, and $\vec{z}'$ with $\vec{z}'$ along [110] or [111]. After the appropriate transformations the results can be compared with the general expressions for the crystal-field-splitting Hamiltonian,

$$\begin{aligned}\mathcal{H}_{\text{stress}}^{\langle 110\rangle}&=\tfrac{1}{8}(C_{11}+2C_{44})PO_2^0-\tfrac{1}{8}(3C_{11}-2C_{44})PO_2^2 \ , \\ \mathcal{H}_{\text{stress}}^{\langle 111\rangle}&=\tfrac{1}{3}C_{44}PO_2^0 \ .\end{aligned} \tag{6}$$

The general form of the second-degree crystal-field Hamiltonian is

$$\mathcal{H}=B_2^0O_2^0+B_2^2O_2^2 \ . \tag{7}$$

This leads to the following relations for the stress-induced crystal-field parameters:

$$\begin{aligned}&B_2^{0\langle 100\rangle}=\tfrac{1}{2}C_{11}P, \quad B_2^{0\langle 110\rangle}=\tfrac{1}{8}(C_{11}+2C_{44})P \ , \\ &B_2^{2\langle 110\rangle}=-\tfrac{1}{8}(3C_{11}-2C_{44})P, \quad B_2^{0\langle 111\rangle}=\tfrac{1}{3}C_{44}P \ .\end{aligned} \tag{8}$$

The values for the B_2^m parameters associated with the various stress directions can be calculated with conventional lattice-sum methods (see Bijvank, den Hartog, and Andriessen,[11] Bijvank and den Hartog,[12] and Roelfsema and den Hartog[1]). Using the theory of elasticity as presented by Geckeler,[13] we can write, for an arbitrary stress direction,

$$\begin{aligned}\epsilon=&\frac{P}{c_{11}-c_{12}}\left[\frac{c_{12}}{c_{11}+2c_{12}}-(m_1^2n_1^2+m_2^2n_2^2+m_3^2n_3^2)\right] \\ &-\frac{P}{c_{44}}(m_1m_2n_1n_2+m_2m_3n_2n_3+m_3m_1n_3n_1) \ ,\end{aligned} \tag{9}$$

where ϵ is the expansion of the sample along an axis with direction cosines m_1, m_2, and m_3 with respect to the principal axes of the crystal. The stress direction has direction cosines n_1, n_2, and n_3. With (9) we can calculate the relative positions of a large number of ions with respect to the origin, which is chosen to coincide with the impurity (Mn^{2+}). We shall refer to the actual positions of the ions in the crystal under stress conditions as $\vec{R}_i'$; the corresponding positions in the unstressed crystal are $\vec{R}_i$.

TABLE II. Theoretical uniaxial-stress effect ($SrCl_2$:Mn^{2+}).

Temperature (K)	B_2^0 (G/kbar) [100]	[110]	[111]	B_2^2 (G/kbar) [100]	[110]	[111]
300	0.42	−0.47	−0.79	0	−0.91	0
0	0.38	−0.43	−0.73	0	−0.83	0

The crystal potential in the neighborhood of the Mn^{2+} ion is expanded in a series of Legendre polynomials, and because we are only interested in second-degree effects, we only keep the second-degree terms,

$$V^{(2)}(\vec{r})=c_2^0(3z^2-r^2)+c_2^2(x^2-y^2)\ . \tag{10}$$

Here, r is the distance from the Mn^{2+} position. In (10) perturbations of the axial and orthorhombic type have been taken into account and the coefficients c_2^0 and c_2^2 can be written as

$$c_2^0=\frac{1}{16\pi\epsilon_0}\sum_i \frac{Q_i(3Z_i'^2-R_i'^2)}{R_i'^5}\ ,$$
$$c_2^2=\frac{3}{16\pi\epsilon_0}\sum_i \frac{Q_i(X_i'^2-Y_i'^2)}{R_i'^5}\ . \tag{11}$$

Here, Q_i is the charge of ion i. For rapid convergence we have calculated the sums by including the contributions of complete unit cells (of 12 ions).

We know that the lattice sums (11) vanish if we take, for the positions of the ions, the unperturbed lattice sites, because of the cubic site symmetry. We have found that the convergence is improved significantly if the lattice sums associated with cubic symmetry are subtracted from the contributions shown in Eq. (11). Thus,

$$c_2^0=\frac{1}{16\pi\epsilon_0}\sum_i Q_i\left[\frac{3Z_i'^2-R_i'^2}{R_i'^5}-\frac{3Z_i^2-R_i^2}{R_i^5}\right],$$
$$c_2^2=\frac{3}{16\pi\epsilon_0}\sum_i Q_i\left[\frac{X_i'^2-Y_i'^2}{R_i'^5}-\frac{X_i^2-Y_i^2}{R_i^5}\right]. \tag{12}$$

From the parameters c_2^0 and c_2^2 one can calculate the theoretical splitting parameters occurring in the stress-induced spin Hamiltonian, $(B_2^0)_{\text{stress}}$ and $(B_2^2)_{\text{stress}}$ (see Hagston and Lowther[14]),

$$B_2^m=\frac{1}{125}\frac{-\xi e c_2^m}{W_P}(-4R_{++}^2+3R_{+-}^2+R_{--}^2)\ , \tag{13}$$

where ξ (the spin-orbit—coupling constant) is 260 cm^{-1}, $W_P=30\,500$ cm^{-1}, and the relativistic integrals R_{++}, R_{+-}, and R_{--} calculated by van Heuvelen[15] lead to $-4R_{++}^2+3R_{+-}^2+R_{--}^2=-0.0485a_0^2$ (a_0 is the Bohr radius). Using these values, we find

$$B_2^m=(7.98\times10^{-19})c_2^m\ . \tag{14}$$

In (14) the c_2^m parameter is given in V/m^2 and B_2^m in G. In the calculations we have taken into account the contributions of 10^5 ions; in addition, we improved the results considerably by employing the trend of the convergence. For the elastic parameters c_{11}, c_{12}, and c_{44} we have taken the values of Lauer, Solberg, Kühner, and Bron;[5] values for 300 and 0 K are available and the results of the calculations based on these values have been listed in Table II. Similar calculations have been carried out for the system SrF_2:Mn^{2+}, and a compilation of the results have been given in Table III; for SrF_2 the elastic parameters at 300, 77, and 0 K are available.[16] We note that the elastic constants at 0 K have been obtained by extrapolation. The C_{11} and C_{44} parameters calculated from the results in Tables II and III have been compiled in Table IV.

The experimental results provide us with values for the stress-induced parameters. These parameters have been compiled in Table V and should be compared with the theoretical results reviewed in Tables II and IV. We see that especially the C_{44} parameter shows a discrepancy and the C_{11} parameter calculated from the deformed lattice has the correct order of magnitude. It should be realized, on the other hand, that the parameters calculated with formula (14) are usually too small by a factor of 2—3.[14] This may be due to the inaccuracy of the theoretical parameters occurring in (13), but another possibility is that the coupling mechanism employed here is not the only one active. There is evidence that the latter is true.[17] Even if we apply a correction factor of about 2.5, it is not possible to obtain agreement between the theoretical and experimental stress-induced parameters.

In order to improve the agreement between theory and experiment we propose that the local elastic constants in the neighborhood of the Mn^{2+} impurity may be different from the bulk values. This is not an unreasonable assumption because the Mn^{2+} ion is appreciably smaller than the host Sr^{2+} ions. Hess and den Hartog[4] have found that the potential well seen by the chloride ions neighboring the Mn^{2+} impurity is appreciably shallower

TABLE III. Theoretical uniaxial-stress effect (SrF_2:Mn^{2+}).

Temperature (K)	B_2^0 (G/kbar) [100]	[110]	[111]	B_2^2 (G/kbar) [100]	[110]	[111]
300	0.48	−0.18	−0.40	0	−0.66	0
77	0.47	−0.17	−0.39	0	−0.65	0
0	0.47	−0.17	−0.39	0	−0.64	0

TABLE IV. Theoretical parameters C_{11} and C_{44} of $SrCl_2:Mn^{2+}$ and $SrF_2:Mn^{2+}$.

Sample	T (K)	C_{11} (G/kbar)	C_{44} (G/kbar)
$SrCl_2:Mn^{2+}$	300	0.75	−2.18
	0	0.84	−2.37
$SrF_2:Mn^{2+}$	300	0.95	−1.20
	77	0.94	−1.17
	0	0.94	−1.16

TABLE V. Experimental uniaxial-stress results of $SrCl_2:Mn^{2+}$.

Stress direction	B_2^0 (G/kbar)	B_2^2 (G/kbar)
[100]	<0.2	0
[110]	±12.3	±12.3
[111]	±13.7	0
	C_{11} (G/kbar)	C_{44} (G/kbar)
	<0.4	±46

than that of the Cl^- ions neighboring host ions only. For these reasons we have taken smaller values for c_{11}, c_{12}, and c_{44}, and it turns out that reduction of c_{11} does not improve the agreement between theory and experiment. It leads to an increase of the parameter C_{11} and it does not influence the results for C_{44}. In terms of the B_2^0 and B_2^2 parameters, reduction of the c_{11} elastic constant gives rise to larger values of $B_2^{0\langle 001\rangle}$. From the results given in Table V we conclude that probably the c_{11} parameter in the neighborhood of the Mn^{2+} impurity is not much different from the bulk one. A similar effect has been observed for c_{12}. Variation of the elastic constant leads to an increase of the parameter C_{44}, and, as a consequence, to increased values of $B_2^{0\langle 110\rangle}$, $B_2^{2\langle 110\rangle}$, and $B_2^{0\langle 111\rangle}$, just as observed experimentally.

In Table VI we have compiled the calculated values of the stress-induced spin-Hamiltonian parameters for reduction factors of $\frac{1}{3}$ and $\frac{1}{10}$. A comparison of the results presented in this table, realizing, as mentioned above, that the theoretical values for the crystal-field parameters are a factor of 2–3 too small, leads to the conclusion that the reduction factor should be about $\frac{1}{5}$.

B. $SrCl_2:Eu^{2+}$

The experimental results for crystals doped with divalent europium can be treated in a way similar to the ones described above and employed to understand the stress-induced splitting parameters. Instead of formula (14) we have to use an alternative formula to account for the coupling between the $^8S_{7/2}$ ground state and the excited states. In accordance with Hutchison, Judd, and Pope,[18] and Wybourne,[19] we write, for the splitting parameters $B_2^m (m=0 \text{ and } 2)$,

$$B_2^m = \left[-\frac{4}{5}\frac{\xi^3}{W_P^2 W_D}\langle r^2\rangle + \frac{16}{735}\frac{\xi}{W_P}\langle R^2\rangle \right] \gamma_2(-e)c_2^m \, . \tag{15}$$

Here, W_p and W_D are the energy separations between the $^8S_{7/2}$ state and the $^6P_{7/2}$ and $^6D_{7/2}$ states, respectively. γ_2 is the screening factor and $\langle r^2\rangle$ is the average of the operator r^2. The matrix element $\langle R^2\rangle$ is a sum of relativistic integrals,

$$\langle R^2\rangle = -5R^2_{++} + 3R^2_{+-} + 2R^2_{--} \, , \tag{16}$$

which have been given by Wybourne[19] and we take $\langle R^2\rangle$ to be equal to $-0.084a_0^2$.[10] In addition, we choose for the parameters occurring in (15), $\xi = 1316\ \text{cm}^{-1}$, $W_P = 29\,400\ \text{cm}^{-1}$, $W_D = 32\,000\ \text{cm}^{-1}$, $\langle r^2\rangle = 0.938a_0^2$, and $\gamma_2 = 0.33$ (see also Wever and den Hartog[21]). Substituting this into formula (15) we find, for Eu^{2+},

$$B_2^m = (11.4\times 10^{-18})c_2^m \, G \, , \tag{17}$$

where c_2^m is given in units of V/m^2. A comparison of Eqs. (14) and (17) shows that Eu^{2+} is far more sensitive to electrostatic potentials that Mn^{2+}, even if we assume that the left-hand side of Eq. (14) has to be multiplied by a factor of 2–3 in order to correct for the discrepancy between theory and experiment as observed by Hagston and Lowther.[14]

As Eu^{2+} is slightly larger than Sr^{2+}, it is reasonable to assume that the potential well "seen" by the Cl^- ions neighboring the Eu^{2+} impurity in $SrCl_2$ or SrF_2 is not much different from that of the ions neighboring the host Sr^{2+} ions. If there is an effect due to the ion size, it will probably lead to slightly larger local elastic constants. As a consequence, the stress-induced parameters will be less than expected on the basis of the bulk properties. In Table VII we have also compiled some results for Eu^{2+} impurities in $SrCl_2$ and SrF_2. Except for the discrepancy obtained for the C_{11} parameter of the system $SrF_2:Eu^{2+}$, we find that the agreement between theory and experiment is better for the Eu^{2+} than for the Mn^{2+} impurities.

In addition, the temperature dependence of the uniaxial-stress effect of $SrCl_2:Eu^{2+}$ is quite different from what is observed for $SrCl_2:Mn^{2+}$. It turns out to be approximately constant in the temperature range investigated, indicating that the anharmonic effects, which have been observed for $SrCl_2:Mn^{2+}$, are not important for $SrCl_2:Eu^{2+}$.

C. $SrCl_2:Co^{2+}$

Unfortunately it is not possible to investigate the uniaxial-stress effect of $SrCl_2:Co^{2+}$ over a wide range of temperatures because for temperatures above 4.2 K the spin-relaxation time decreases very rapidly with increasing temperature. The results at 4.2 K are, however, very interesting. Firstly, because the observed stress-induced crystal-field splitting is very large, and secondly, because with increasing stress the relative intensities of the fine transitions vary drastically.

The magnitude of the stress-induced crystal-field parameters can be calculated along lines which are about the same as those for $SrCl_2:Mn^{2+}$ and $SrCl_2:Eu^{2+}$. The prob-

TABLE VI. Theoretical stress-induced parameters employing a reduced value of c_{44} for the eight Cl^- ions neighboring the Mn^{2+} impurity.

Reduction factor	B_2^0 (G/kbar) [100]	[110]	[111]	B_2^2 (G/kbar) [100]	[110]	[111]
$\frac{1}{3}$	0.38	−1.81	−2.66	0	−2.28	0
$\frac{1}{10}$	0.38	−6.47	−10.07	0	−7.83	0

lem is, however, that the coupling mechanisms, which relate the electrostatic crystal-field potential with the splitting of the magnetic energy levels, are unknown for Co^{2+}. In Fig. 14 we give the energy-level diagram of divalent cobalt in $SrCl_2$, and it can be seen that the ground state is a quartet state, which can be considered an effective $S=\frac{3}{2}$ state with $L=0$. Because the excited states are relatively close to this level there is a strong admixture of the excited-state wave function into the ground-state wave function. This explains the very large splitting associated with the electrostatic crystal-field potential. Another reason for the very large uniaxial-stress effect may be the fact that the Co^{2+} ion is smaller than the Mn^{2+} ion. It is expected that the above-mentioned anharmonic contributions to the potential well of Co^{2+} in the $SrCl_2$ lattice are stronger than for the system $SrCl_2$:Mn^{2+}. In addition, it can be understood that the electric field effect, as observed by Roelfsema and den Hartog,[1] is very large even at temperatures as low as 4.2 K.

From the results of the uniaxial-stress effect obtained for $SrCl_2$:Co^{2+} at 4.2 K (see Table I), we see that there is, apart from the magnitude of the crystal-field parameters, a major difference as compared to the results obtained for $SrCl_2$:Mn^{2+}. The ratio of the parameters C_{11} and C_{44} is quite different from the one observed for $SrCl_2$:Mn^{2+}. For $SrCl_2$:Co^{2+} the value of C_{11} is relatively large, indicating that the local distortions during the application of uniaxial stress along the ⟨100⟩ directions are large. For the system $SrCl_2$:Mn^{2+} we have concluded that only the local elastic constant c_{44} of the neighboring Cl^- ions is reduced. In the present case ($SrCl_2$:Co^{2+}) we must conclude that the value of c_{11} is also reduced significantly.

V. SUMMARY AND CONCLUSIONS

Comparing the uniaxial-stress results obtained for the different samples studied in this paper, we conclude that the size of the impurities is a very important parameter, one that determines the magnitude of the uniaxial-stress effect. The uniaxial-stress effect observed for the system $SrCl_2$:Eu^{2+} can be explained fairly well by the distortions expected from the bulk elastic properties of the $SrCl_2$ lattice. Furthermore, the behavior of the uniaxial-stress effect as a function of the temperature is as expected.

A completely different situation has been observed for $SrCl_2$:Mn^{2+}. Here the uniaxial-stress effect for applied stress along ⟨111⟩ axes is appreciably larger than expected on the basis of the bulk elastic properties of the pure $SrCl_2$ crystal. This can be explained by assuming that the force constants of the Cl^- ions surrounding the relatively small Mn^{2+} impurity are significantly smaller than those of the Cl^- ions surrounding a Sr^{2+} ion. This is supported by results of calculations carried out earlier in our laboratory (Hess and den Hartog[4]).

The behavior of the uniaxial-stress effect as a function of the temperature observed for $SrCl_2$:Mn^{2+} is anomalous. This can be explained by assuming that the potential well of the Mn^{2+} impurity is highly anharmonic. In addition, we must assume that the potential well is very shallow. Theoretically, we have also found these features (see Hess and den Hartog[4]). With increasing temperatures the amplitude of the motion of the Mn^{2+} ion increases significantly because excited vibrational states are being occupied (also see Fig. 1). The corresponding variations of the crystal-field-splitting parameters are very large compared to what has been observed for normal Mn^{2+}-doped samples.[7] In addition, the temperature range in which these

TABLE VII. Experimental and theoretical uniaxial-stress results of $SrCl_2$:Eu^{2+} and SrF_2:Eu^{2+}.

Sample	$\lvert C_{11}\rvert$ (G/kbar) Expt.	theory	$\lvert C_{44}\rvert$ (G/kbar) Expt.	theory
$SrCl_2$:Eu^{2+}	1	12.0	9	33.9
SrF_2:Eu^{2+}	3.9[a]	13.6	9.7[a]	17.1

[a] See Ref. 22.

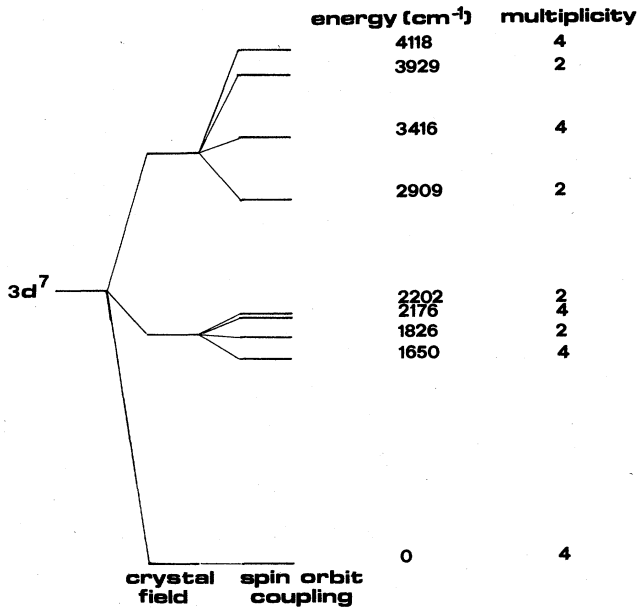

FIG. 14. Energy-level diagram of divalent cobalt in $SrCl_2$.

large variations are observed is limited, which is also in contrast with the results obtained for normal Mn^{2+}-doped samples.

The results obtained for $SrCl_2$:Co indicate that there is a very strong admixture of excited states into the ground-state level. From a detailed investigation of the uniaxial-stress effect as a function of the stress direction we conclude that the local elastic constants in the neighborhood of the small-sized Co^{2+} impurity is modified significantly with respect to the bulk values. Both c_{11} and c_{44} have been reduced significantly. It is suggested that the anharmonic effects due to the difference between the ionic radii of Sr^{2+} and Co^{2+} are stronger than in the system $SrCl_2$:Mn^{2+}. Unfortunately, the EPR experiments on $SrCl_2$:Co^{2+} can only be carried out in a very limited temperature range.

[1]K. E. Roelfsema and H. W. den Hartog, Phys. Rev. B **13**, 2723 (1976).
[2]K. E. Roelfsema and H. W. den Hartog, J. Magn. Reson. **29**, 255 (1978).
[3]J. A. van Winsum, H. W. den Hartog, and T. Lee, Phys. Rev. B **18**, 178 (1978).
[4]F. Hess and H. W. den Hartog, in *Recent Developments in Condensed Matter Physics,* edited by J. T. Devreese, L. F. Lemmens, V. E. van Doren, and J. van Royen (Plenum, New York, 1981), Vol. 3.
[5]H. W. Lauer, K. A. Solberg, D. H. Kuhner, and W. E. Bron, Phys. Lett. **35**, 219 (1971).
[6]J. Szumowski and K. Falkowski, Rev. Sci. Instrum. **47**, 252 (1976).
[7]G. Pfister, W. Dreybrodt, and W. Assmus, Phys. Status Solidi **36**, 351 (1969).
[8]E. A. Harris and J. W. Tucker, Phys. Status Solidi B **117**, 301 (1983).
[9]R. G. Shulman, B. S. Wykeda, and P. W. Anderson, Phys. Rev. **107**, 953 (1951).
[10]E. Rosenvasser Feher, Phys. Rev. **136**, A145 (1964).
[11]E. J. Bijvank, H. W. den Hartog, and J. Andriessen, Phys. Rev. B **16**, 1008 (1977).
[12]E. J. Bijvank and H. W. den Hartog, Phys. Rev. B **22**, 4133 (1980).
[13]J. W. Geckeler, *Handbuch der Physik VI* (Springer, Berlin, 1927), pp. 404—427.
[14]W. E. Hagston and J. E. Lowther, J. Phys. Chem. Solids **34**, 1773 (1973).
[15]A. van Heuvelen, J. Chem. Phys. **46**, 4903 (1967).
[16]W. Hayes, *Crystals with the Fluorite Structure* (Clarendon, Oxford, 1974).
[17]D. J. Newman and W. Urban, Adv. Phys. **24**, 793 (1975).
[18]C. A. Hutchison, B. R. Judd, and D. F. D. Pope, Proc. Phys. Soc. London, Sect. B **70**, 514 (1957).
[19]B. G. Wybourne, Phys. Rev. **148**, 317 (1966).
[20]J. I. Waber and D. T. Cromer, J. Chem. Phys. **42**, 4116 (1965).
[21]H. Wever and H. W. den Hartog, Phys. Status Solidi B **70**, 253 (1975).
[22]D. Zadunaisky de Basch and G. E. Barberis, Solid State Commun. **18**, 1439 (1976).